

Magnetic Monopole Interactions: Shell Structure of Meson and Baryon States

David Akers^{1,2}

Received December 16, 1985

It is suggested that a low-mass magnetic monopole of Dirac charge $g = (137/2)e$ may be interacting with a c -quark's magnetic dipole moment to produce Zeeman splitting of meson states. The mass $M_0 = 2397$ MeV of the monopole is in contrast to the 10^{16} -GeV monopoles of grand unification theories (GUT). It is shown that shell structure of energy $E_n = M_0 + \frac{1}{4}nM_0 + \dots$ exists for meson states. The presence of symmetric meson states leads to the identification of the shell structure. The possible existence of the 2397-MeV magnetic monopole is shown to quantize quark masses in agreement with calculations of quantum chromodynamics (QCD). From the shell structure of meson states, the existence of two new mesons is predicted: $\eta(1814 \pm 50 \text{ MeV})$ with $I^G(J^{PC}) = 0^+(0^{-+})$ and $\eta_c(3907 \pm 100 \text{ MeV})$ with $J^{PC} = 0^{-+}$. The presence of shell structure for baryon states is shown.

1. INTRODUCTION

There is evidence (Akers, 1985) that a low-mass magnetic monopole of Dirac charge $g = (137/2)e$ may be Zeeman-splitting meson states. This evidence is presented in Section 2. In Section 3 we present evidence of shell structure and quantization of quark masses; these masses are not accounted for until now. While grand unification theories (GUT) predict massive 10^{16} -GeV monopoles (Liss *et al.*, 1984), few theorists study low-mass magnetic monopoles, though early work indicated a monopole mass of $2.5M_p$ (Amaldi, 1968). No improvement on the classical Dirac mass has occurred since 1968, attention having focused on the massive 10^{16} -GeV monopoles of GUT. Lochak (1985) has studied the low-mass end of the spectrum and found a massless monopole from the Dirac wave equation. In this paper, we return to the Dirac mass of 2397 MeV and find evidence to support the existence of the magnetic monopole.

¹Bethany Bible College, Santa Cruz, California 95066.

²Permanent Address: 20970 Pawnee Trail, Los Gatos, California 95030.

2. ZEEMAN SPLITTING

First, we recall that the mass of the magnetic monopole can be estimated on the basis of magnetic self-interaction (Barut, 1979; Salam and Tiomno, 1959; Stephenson, 1957):

$$M = \frac{g^2}{e^2} m_e \quad (1)$$

where g is the magnetic charge of the monopole, e is the electric charge, and m_e is the electron mass. The quantization condition (Dirac, 1931) is

$$ge = \frac{1}{2} n \hbar c, \quad n = 0, \pm 1, \dots \quad (2)$$

The trivial case $n = 0$ corresponds to a massless magnetic monopole whose properties can be derived from the Dirac equation (Lochak, 1985). We concern ourselves with the first magnetic monopole mass for $n = 1$:

$$M = (137/2)^2 m_e = 2397 \text{ MeV} \quad (3)$$

which is the Dirac mass. We shall reconcile the existence of a 2397-MeV monopole with grand unification theories. This development will be discussed in Section 4 on the theory of strong forces.

Drawing from the abundance of evidence for charmonium states (Particle Data Group, 1984), we plot the energy levels for $I = 0$ mesons in Figure 1. The charmonium states are located above the 2397-MeV Dirac mass, which is indicated by the dashed line. Below the $M_0 = 2397$ -MeV magnetic monopole, we find energy levels symmetric to the charmonium states. For clarity not all isoscalar mesons are shown in Figure 1. Figure 4 shows all the $I = 0$ mesons. We note the unmistakable symmetry, apparently about $M_0 = 2397$ MeV. The particle masses are shown in parentheses, and the absolute value of the particle-monopole mass difference is in brackets.

Before we discuss Figure 1, a number of comments can be made. First, the evidence of Figure 1 does not exclude the existence of mesons heavier than 4.8 GeV, twice the monopole mass. The monopole also has heavier masses: 9.6 GeV for $n = 2, \dots$. The model may thus be extended to the ϵ family.

Second, the symmetry of Figure 1 is not found for nonisoscalar mesons, because of the limits of present experimental data. However, the symmetry of Figure 1 reveals shell structure (see Section 3), which the nonisoscalar mesons satisfy systematically. Finally, one could argue from a partial wave analysis that there is a continuum of states and that the symmetry claimed would disappear with a more complete knowledge of the meson spectrum. Such an argument does not completely remove the symmetry of Figure 1, but it does introduce an asymmetry into the spectrum. This slight asymmetry

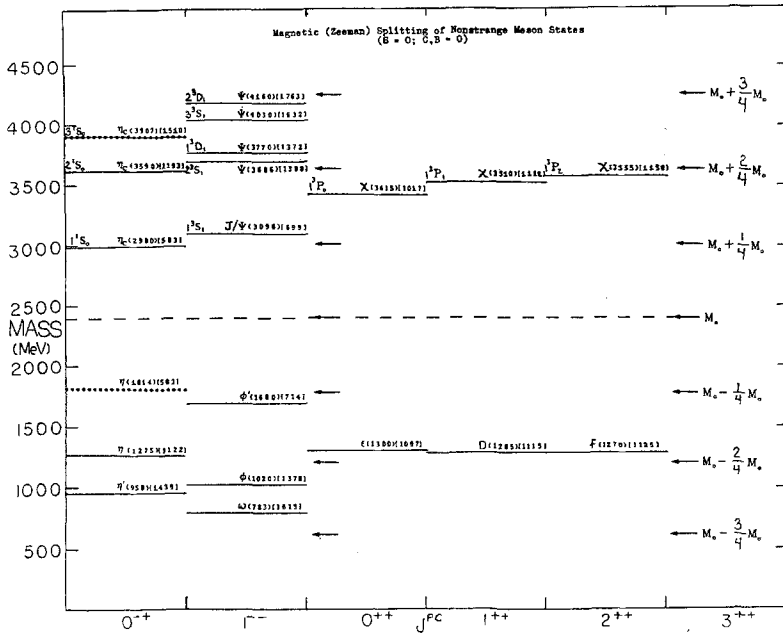


Fig. 1. Combined meson spectrum for isospin $I=0$. The magnetic monopole of mass M_0 is indicated by the dashed line. The arrows point to shell states calculated to first-order approximation, equation (6). The dotted line represents a missing meson at 1814 MeV. We predict another meson at 3907 MeV, as represented by the dotted line.

can be explained from the fact that even in atomic systems there is a slight asymmetry in the Zeeman splitting of the energy levels (Anderson, 1971).

We propose that the symmetry of meson states about $M_0 = 2397$ MeV is due to Zeeman splitting from a quark's magnetic dipole moment interacting with the monopole's B field. The energy of the Zeeman splitting is given by the relation

$$\Delta E = gm_j \mu B \tag{4}$$

where the gm_j factors are shown in Table I and μ is the magnetic dipole moment of a quark. We clarify the nature of the Zeeman effect by defining the relationship between a charmed meson's interactions and a normal meson's interactions with a magnetic monopole. The orientations of magnetic dipole moments μ_s and μ_c with respect to the monopole are given by the relations

$$\Delta E = -\mu_c \cdot \mathbf{B} \text{ for a } c\text{-quark} \tag{5a}$$

$$\Delta E = -\mu_s \cdot \mathbf{B} \text{ for an } s\text{-quark} \tag{5b}$$

Table I. Zeeman Energy Splitting for p and s States

Orbital states	j	m_j	g	$\Delta E = gm_j$ (in units of μB)
p	$\frac{3}{2}$	$\frac{3}{2}$	$\frac{4}{3}$	2
p	$\frac{3}{2}$	$\frac{1}{2}$	$\frac{4}{3}$	$\frac{2}{3}$
p	$\frac{3}{2}$	$-\frac{1}{2}$	$\frac{4}{3}$	$-\frac{2}{3}$
p	$\frac{3}{2}$	$-\frac{3}{2}$	$\frac{4}{3}$	-2
p	$\frac{1}{2}$	$\frac{1}{2}$	$\frac{2}{3}$	$\frac{1}{3}$
p	$\frac{1}{2}$	$-\frac{1}{2}$	$\frac{2}{3}$	$-\frac{1}{3}$
s	$\frac{1}{2}$	$\frac{1}{2}$	2	1
s	$\frac{1}{2}$	$-\frac{1}{2}$	2	-1

From Table I, $gm_j = 1$ for a spin singlet state ($m_j = \frac{1}{2}$), and $gm_j = -1$ for $m_j = -\frac{1}{2}$. For the $\eta_c(2980) - M_0$ mass difference, $gm_j = 1$ and the Zeeman splitting is $\Delta E = -\boldsymbol{\mu}_c \cdot \mathbf{B} = 2980 - 2397 = +583$ MeV, where $\boldsymbol{\mu}_c = +(2e/3m_c c) \mathbf{S}$ and $\mathbf{B} = -(137e/2r^2)\hat{r}$. The meson spectrum is normalized with respect to the spin singlet state of charmonium, and the experimental gm_j factors are shown in Table II. The ratio of the highest p state $\chi(3555)$ and the s state $\eta_c(2980)$ is 1.99, which agrees with the theoretical value of 2 from Table I. Namely, the ratio $[\chi(3555) - M_0]/[\eta_c(2980) - M_0] = 1.99$ is in agreement with $gm_j = 2$ in the p states for Zeeman splitting. The experimental gm_j factors of Table II support the claim for Zeeman splitting in Figure 1.

Table II. Zeeman Splitting for the $1p$ and $1s$ States of Charmonium and of the Symmetric States^a

	1S_0	3S_1	3P_0	3P_1	3P_2
n	1	1	1	1	1
l	0	0	1	1	1
s	0	1	1	1	1
J^-	0	1	0	1	2
Intermediate states					
$j' = l + s'$	1/2	1/2	3/2	3/2	3/2
\vdots			1/2	1/2	1/2
\vdots			-1/2	-1/2	-1/2
$j' = l - s'$	-1/2	-1/2	-3/2	-3/2	-3/2
Charmonium states above $M_0 = 2397$ MeV					
$\eta_c(2980)$		$J(3096)$	$\chi(3415)$	$\chi(3510)$	$\chi(3555)$
gm_j	1.00	1.20	1.74	1.91	1.99
Symmetric states below $M_0 = 2397$ MeV					
$\eta(1814)$		$\phi'(1680)$	$\varepsilon(1300)$	$D(1285)$	$f(1270)$
gm_j	-1.00	-1.22	-1.88	-1.91	-1.93

^a Monopole spin $s' = \frac{1}{2}$ (Osborn, 1982).

Further comment on Table II is needed. Because the gm_j factors vary from 1.74 to 1.99 in the p states above $M_0 = 2397$ MeV and from -1.88 to -1.93 in the p states below M_0 , we suggest an intermediate L - S and j - j coupling with a monopole spin $s' = \frac{1}{2}$ and $j' = l + s', \dots, j' = l - s'$. In fact, the monopole is expected to have a spin (Osborn, 1982). This additional coupling may account for the additional 1^- mesons and for the slight asymmetry in the p states of Figure 1.

Moreover, from the symmetry of Figure 1, we note the mass differences in brackets are very close for each J^{PC} bin. The numbers in brackets are the absolute values of the particle-monopole mass difference. In the p states, there is a slight asymmetry about the monopole mass. Choi (1985) has suggested that the symmetry about the monopole mass M_0 may be broken, since the spin splitting scales of the charmonium and the low-mass meson systems are slightly different in general. This has to be considered as a possible alternative to the intermediate coupling scheme mentioned above. The intermediate coupling scheme seems to be the more reasonable explanation of the slight asymmetry, because a similar asymmetry for Zeeman splitting exists in atomic systems (Anderson, 1971).

In studying Figure 1, we notice that there are two missing η mesons, as indicated by the dotted lines in the $J^{PC} = 0^{-+}$ bin. The $\eta(1814)$ meson is predicted to exist, because it is symmetric with respect to $\eta_c(2980)$. Thus, we predict the existence of a new η meson at 1814 ± 50 MeV with $I^G(J^{PC}) = 0^+(0^{-+})$ and another charmonium singlet state η_c at 3907 ± 100 MeV. These masses are determined by comparison with their symmetric states. Hence, the singlet $\eta_c(3907)$ is a reflection of $\eta(958)$.

In sum, the extent to which the energy splittings in equation (4) are based upon the coupling of a quark to a magnetic monopole remains to be seen. The theory of magnetic monopoles is far enough along that one could explore concrete Schrödinger equations, although the calculations are somewhat complex (Akers and Akers, 1984; Sivers, 1970).

3. SHELL STATES

In the meson spectrum of Figure 1, the energy levels are grouped in shell states according to the first-order approximation:

$$E_n = M_0 + \frac{1}{4}nM_0, \quad n = 0, \pm 1, \dots \quad (6)$$

$M_0 = 2397$ MeV is the monopole mass from equation (3). The 1^1S_0 and 1^3S_1 states of charmonium appear at the $E_1 = M_0 + \frac{1}{4}M_0$ level. Likewise, the 2^1S_0 and 2^3S_1 states also appear at the $E_2 = M_0 + \frac{2}{4}M_0$ shell state. On the other hand, the 3^1S_0 and 3^3S_1 levels fall below the $E_3 = M_0 + \frac{3}{4}M_0$ shell state. This

is expected since equation (6) is a first-order approximation. The correct shell state energy is given by the relation

$$E_3 = M_0 + \frac{3}{4}M_0 - \frac{1}{8}M_0 = 3895 \text{ MeV} \quad (7)$$

Thus, the shell state energy is measured from the spectrum of Figure 1. For those mesons below the Dirac mass, the shell state energies have negative values for n .

A question arises as to whether the symmetry in Figure 1 is due to chance. A statistical analysis of the spin-singlet and spin-triplet states reveals that the symmetry is not due to chance. In Table III, nine of the meson masses are within one standard deviation of the energy levels. Two mesons, $\eta(1275)$ and $\phi(1020)$, are within two standard deviations of the energy levels. Hence, there is a symmetry of the mesons in Figure 1.

From the shell structure of equation (6), a relation can be derived between the monopole mass M_0 and quark masses. The mass of a quark is given by those meson states that ideally satisfy equation (6):

$$E_n = m_q + m_{\bar{q}} \quad (8)$$

where E_n is the approximation (6) and m_q is the mass of a quark q . For the c -quark, $m_c + m_{\bar{c}} = E_0$ or $m_c = \frac{1}{2}M_0$. The next meson state is given by $\phi = s\bar{s}$ for $m_s + m_{\bar{s}} = E_2$ or $m_s = \frac{1}{4}M_0$. Ideally ω gives the meson state for $m_u + m_{\bar{u}} = E_3$ or $m_u = \frac{1}{8}M_0$. The results for all quark masses are calculated in Table IV. The ω is not a pure $u\bar{u}$ or $d\bar{d}$ state; since $\omega = 2^{-1/2}(u\bar{u} + d\bar{d})$, $m_u = (1/8\sqrt{2})M_0$ would be more exact. In Table IV, the magnetic monopole model is compared with several quantum chromodynamic (QCD) models. The QCD calculations of (Lizzi and Rosenzweig (1985) are compared with the magnetic monopole model. Moreover, the model is compared with the

Table III. Statistical Analysis of Spin-Singlet and Spin-Triplet States

Energy level (MeV)	1S_0	ΔE (MeV)	3S_1	ΔE (MeV)
$E_3 = 3895.0$	3907	-12.0	4030	135.0
$E_2 = 3595.5$	3590	5.5	3686	90.5
$E_1 = 2996.3$	2980	16.3	3096	99.7
$M_0 = 2397.0$	—	—	—	—
$E_1 = 1797.8$	—	—	1680	117.8
$E_2 = 1198.5$	1275	76.5	1020	178.5
$E_3 = 898.8$	958	59.1	783	115.9
Mean		29.1		122.9
σ		37.3		31.3

Table IV. The Magnetic Monopole Model Fits to the Quark Model of Quantum Chromodynamics (QCD)

Magnetic-monopole model	QCD model
$m_{u,d} = \frac{1}{8}M_0 = 299.5 \text{ MeV}$	$300,^a 330,^b 270 \text{ MeV}^d$
$m_s = \frac{1}{4}M_0 = 599 \text{ MeV}$	$450,^a 450,^b 630 \text{ MeV}^d$
$m_c = \frac{1}{2}M_0 = 1.2 \text{ GeV}$	1.2GeV^c
$m_0 = M_0 = 2.4 \text{ GeV}$	—
$m_b = 2M_0 = 4.79 \text{ GeV}$	4.78 GeV^c

^aRegge trajectories analysis of QCD confinement model (Lizzi and Rosenzweig, 1985).

^bQCD spin-dependent forces model (Choi, 1985, and personal communication).

^cQCD Gupta-Radford model (Gupta *et al.*, 1985).

^dNonrelativistic potential model (Henriques, 1983).

QCD spin-dependent forces model of Choi (1985), the QCD Gupta-Radford model (Gupta *et al.*, 1985), and a nonrelativistic potential model (Henriques, 1983). These quark models agree very well with the magnetic monopole model. The existence of a magnetic monopole implies the quantization of quark masses:

$$m_{u,d} = 300 \text{ MeV}, \quad m_s = 600 \text{ MeV}, \quad m_c = 1.2 \text{ GeV}, \quad m_b = 4.8 \text{ GeV} \quad (9)$$

No research has ever before accounted for quark masses. QCD calculations are long and difficult to perform, whereas the quark masses are easily obtained from the shell structure, equation (6).

Further analysis of the shell structure can be applied systematically to nonisoscalar mesons as well. From the shell state energies of equation (6), the meson masses are plotted for isospins $I = 0, \frac{1}{2},$ and 1. These meson masses are shown in Figures 2–4 and are plotted against $|n|$ of equation (6) for convenience. For $I = 1$ mesons of Figure 2, there are clearly three groups of particles, or shell states, at $|n| = 0, 1,$ and 2. These groups of particles are separated by gaps as indicated. At $|n| = 0,$ the $I = 1$ mesons have large values of angular momentum ($J = 1, \dots, 6$) near the monopole mass $M_0.$ At $|n| = 1,$ the mesons have $J = 0, \dots, 3,$ whereas at $|n| = 2, J = 0, \dots, 2.$ The linearity of equation (6) breaks down at $|n| = 3$ as mentioned earlier. For the $I = \frac{1}{2}$ mesons of Figure 3, the same pattern of large J values appears near M_0 for $|n| = 0,$ and the shell states appear for $|n| = 1$ and 2. Intermediate states K^* with $J^p = 1^-$ and L with $J^p = 2^-$ appear between the $|n| = 1$ and 2 shell states. For the $I = 0$ mesons of Figure 4, there is the same pattern of shell structure. Intermediate states $D(1530), f'(1525), i(1440),$ and $E(1420)$ appear between the $|n| = 1$ and 2 shell states; these intermediate

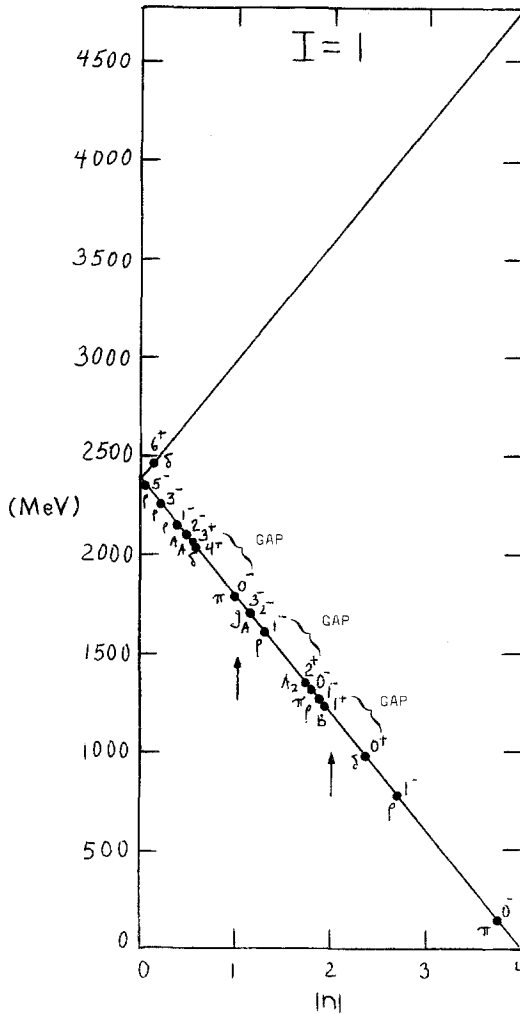


Fig. 2. $I = 1$ meson masses as a function of $|n|$ from equation (6).

states are explainable from Table II. In Table II, the intermediate states are represented by the couplings $j' = l + s', \dots, j' = l - s'$. These intermediate states are likely from the intermediate coupling for j' . In sum, the shell structure, equation (6), can be applied to nonisoscalar mesons as well as to $I = 0$ mesons.

Finally, we look at the possibility of shell structure for baryon states that depend upon the monopole mass M_0 . The evidence for this is not very convincing because of the limited experimental data above the monopole

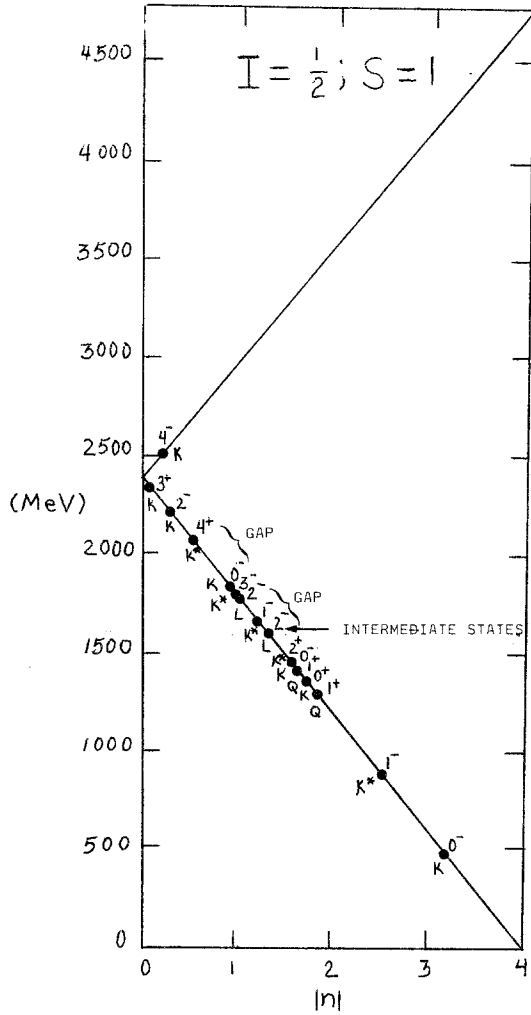


Fig. 3. $I = \frac{1}{2}$ meson masses as a function of $|n|$ from equation (6).

mass $M_0 = 2397$ MeV. The results are shown in Figures 5 and 6, where the absolute value of the monopole-baryon mass difference is plotted against baryon mass. In Figure 5, there may be evidence for shell states symmetric about the Dirac mass. There are clearly groups of particles below the mass M_0 . In Figure 6, the evidence is not convincing enough; however, the particle spectrum is similar to that in Figure 5, with some groups of particles below M_0 . Thus, the presence of shell structure for baryon states based on the monopole mass is not established as yet.

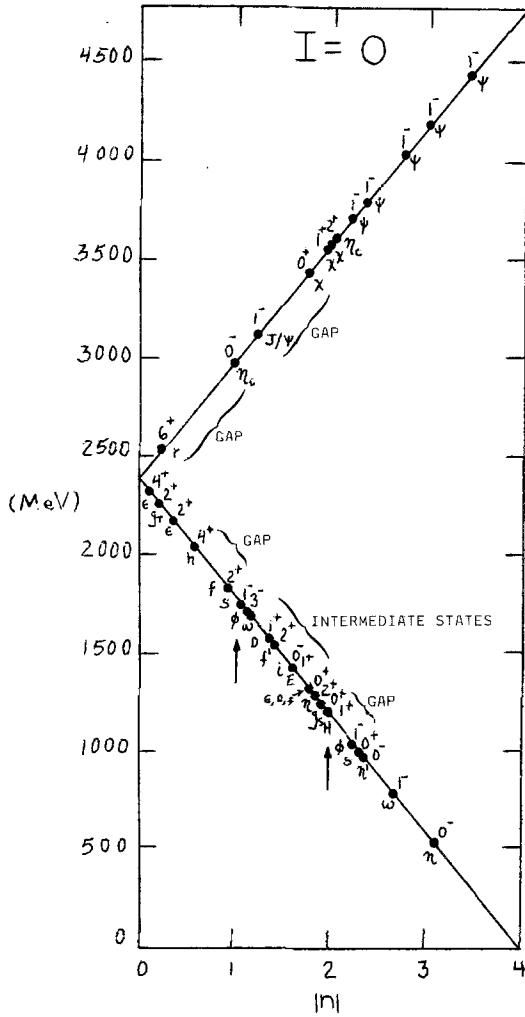


Fig. 4. $I=0$ meson masses as a function of $|n|$ from equation (6).

4. MAGNETOSTRONG THEORY

From the possibility that a low-mass monopole does exist, we shall attempt to reconcile its existence with grand unification theories (GUT). A new unification theory of the magnetic and the strong forces is proposed. The existence of a magnetic monopole is incorporated into the theory. Magnetostromg theory is the idea that the existence of magnetic monopoles accounts for the strong forces in nature. In electron-positron annihilation,

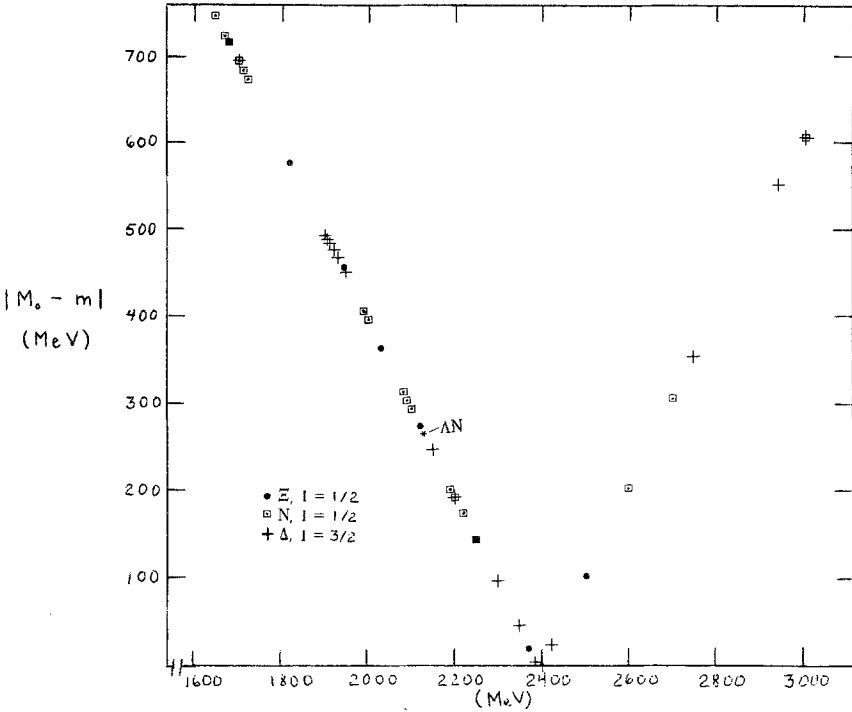


Fig. 5. Baryon shell structure for $I = 1/2, 3/2$.

monopole-antimonopole pairs may be created:

$$e^+ e^- \rightarrow g^+ g^- \tag{10}$$

If the monopole-antimonopole pair is created from vacuum, $\Delta E = 2M_0$, the mean lifetime is $\Delta t \sim \hbar/\Delta E = 1.4 \times 10^{-25}$ sec. The hadron interactions are 100 times longer at $t \sim 10^{-23}$ sec. Therefore, the creation of monopoles involves superstrong forces, as its coupling constant suggests; $\alpha_g = g^2/\hbar c = 34.25$ (for $n = 1$). Hence, the strength of the magnetic charge may account for the confinement of quarks (Daniel *et al.*, 1980).

The nature of the strong coupling constant α_s can be derived from quantum mechanical principles. By considering the interactions as in equation (10), α_s is calculated from the Zeeman splitting. The interaction energy is $\Delta E = -\mu_j \cdot \mathbf{B}$, where $\mu_j = \mu_L + \mu_S$ is the magnetic dipole moment of the system; taking the reduced mass $\frac{1}{2}M$ into account, we have

$$\Delta E = -\frac{Q\hbar}{2M_0c} \frac{137}{2} e \frac{1}{\hbar} \frac{L+2S}{r^2} \cdot \hat{\mathbf{r}} \tag{11}$$

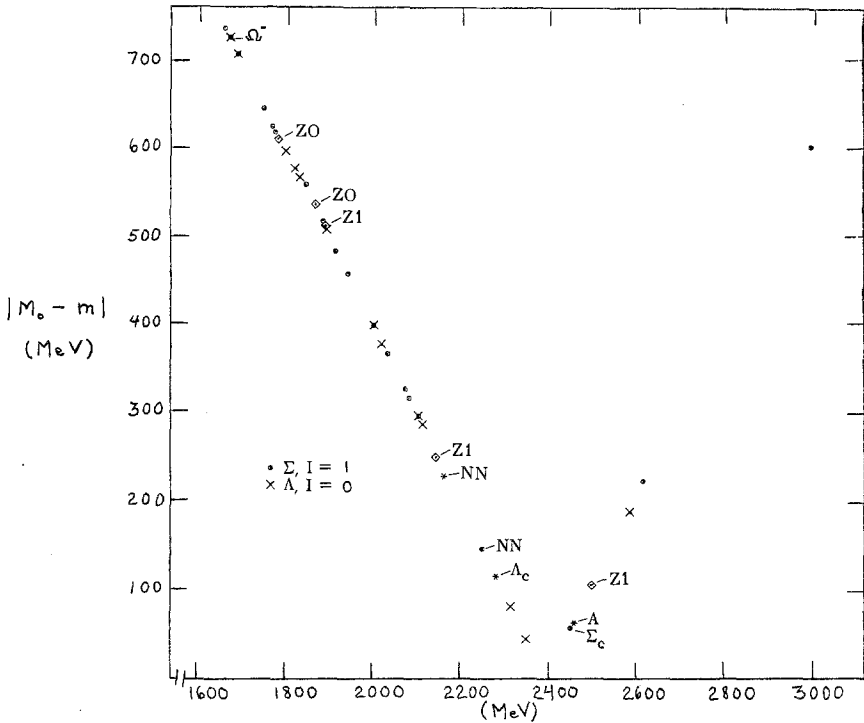


Fig. 6. Baryon shell structure for $I=0, 1$.

where $Q = 2e/n$. The strong coupling constant is then

$$\alpha_s = \frac{Q^2(137e)^2}{\hbar c^2} \frac{1}{\hbar c} \tag{12}$$

and $\alpha_s = 1.0, 0.25, 0.11, \dots$ for $n = 1, 2, \dots$. For $n = 0$, $\alpha_s \rightarrow \infty$ at the low-energy limit, as expected. The center-of-mass energy is given by

$$E = 2M = 2M_0 n^2 \tag{13}$$

In Figure 7, the strong coupling constant is plotted as a function of the center-of-mass energy. From the figure, we note that the magnetostong theory agrees with several experimental measurements (Zhu, 1985). At low energies, there is need for further measurements to confirm the theory or to determine if the theory needs improvement in modeling.

5. CONCLUSION

Finally, we reconcile grand unification theory with a low-mass magnetic monopole. We evaluate the electroweak theory's coupling constant α_w and

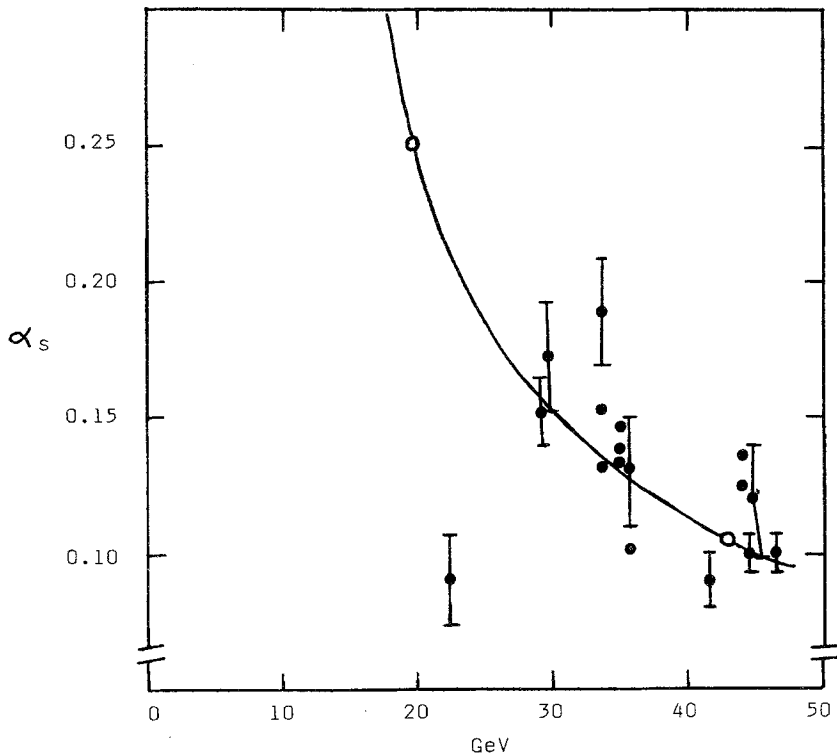


Fig. 7. The strong coupling constant α_s as a function of the center of mass energy. The open circles and curve are from magnostromg theory and the solid points from experimental measurements (Zhu, 1985).

the magnostromg theory's α_s in equation (12) together. The weak coupling constant is given by (Perkins, 1982)

$$\alpha_w = 1.02 \times 10^{-5} (M_w/M_p)^2 \quad (14)$$

where $M_p = 0.938$ GeV. For $\alpha_s = \alpha_w$, $M_w = 73.4$ GeV. For $n = 4$, $\alpha_s = 0.0625$ and $E = 76.7$ GeV. M_w and E agree to within 4%. Hence, the strong, weak, and electromagnetic couplings converge at the intermediate vector boson mass M_w . The model presented in this paper predicts grand unification at the low-energy end of the spectrum. This is to be expected, since we believe the magnetic monopole to have the classical Dirac mass instead of the massive 10^{16} GeV of grand unification theories. The next generation of particle accelerators should decide the issue concerning the existence of magnetic monopoles and their mass.

ACKNOWLEDGMENT

Part of the research in this paper was presented in a talk at the Annual Meeting of the Division of Particles and Fields, University of Oregon, Eugene, Oregon, August 15, 1985.

REFERENCES

- Akers, D. (1985). In *Proceedings of the Oregon Meeting*, Rudolph C. Hwa, ed., World Scientific, Singapore.
- Akers, D., and Akers, D. O. (1984). *Physical Review D*, **29**, 1026.
- Amaldi, E. (1968). In *Old and New Problems in Elementary Particles*, G. Puppi, ed., Academic Press, New York.
- Anderson, E. (1971). *Modern Physics and Quantum Mechanics*, W. B. Saunders, Philadelphia.
- Barut, A. O. (1979). *Physical Review Letters*, **42**, 1251.
- Choi, J. B. (1985). *Physical Review D*, **31**, 201.
- Daniel, M., Lazarides, G., and Shafi, Q. (1980). *Nuclear Physics B*, **170**, 156.
- Dirac, P. A. M. (1931). *Proceedings of the Royal Society of London, Series A*, **133**, 60.
- Gupta, S., Radford, S., and Repko, W. (1982). *Physical Review D*, **26**, 3305.
- Henriques, A. B. (1983). *Zeitschrift für Physik C*, **18**, 213.
- Liss, T. M., Ahlen, S. P., and Tarle, G. (1984). *Physical Review D*, **30**, 884.
- Lizzi, F., and Rosenzweig, C. (1985). *Physical Review D*, **31**, 1685.
- Lochak, G. (1985). *International Journal of Theoretical Physics*, **24**, 1019.
- Osborn, H. (1982). *Physics Letters*, **115B**, 226.
- Particle Data Group. (1984). *Review of Modern Physics*, **56**, S181.
- Perkins, D. H. (1982). *Introduction to High Energy Physics*, Addison, London.
- Salam, A., and Tiomno, J. (1959). *Nuclear Physics* **9**, 585.
- Sivers, D. (1970). *Physical Review D*, **2**, 2048.
- Stephenson, G. (1957). *Nuovo Cimento*, **5**, 1009.
- Zhu, R. (1985). In *Proceedings of the Oregon Meeting*, Rudolph C. Hwa, ed., World Scientific, Singapore.